frontiers | Frontiers in Chemistry

TYPE Original Research
PUBLISHED 09 January 2023
DOI 10.3389/fchem.2022.990979

OPEN ACCESS

EDITED BY
Pedro Vaz,
Champalimaud Foundation, Portugal

REVIEWED BY
Kang-Nan Wang,
Shandong University, China
Qiu-Juan Ma,
Henan University of Traditional Chinese Medicine, China

*CORRESPONDENCE
Y. J. Peng,
hunterpyj2016@163.com

SPECIALTY SECTION
This article was submitted to Theoretical and Computational Chemistry, a section of the journal Frontiers in Chemistry

RECEIVED 11 July 2022
ACCEPTED 14 December 2022
PUBLISHED 09 January 2023

CITATION
Lin XY, Sun SH, Liu YT, Shi QQ, Lv JJ and Peng YJ (2023), Thiophene and diaminobenzo- (1,2,5-thiadiazol)- based DAD-type near-infrared fluorescent probe for nitric oxide: A theoretical research. *Front. Chem.* 10:990979.
doi: 10.3389/fchem.2022.990979

Thiophene and diaminobenzo- (1,2,5-thiadiazol)- based DAD-type near-infrared fluorescent probe for nitric oxide: A theoretical research

X. Y. Lin[1], S. H. Sun[1], Y. T. Liu[1], Q. Q. Shi[1], J. J. Lv[1] and Y. J. Peng[2,3]*

[1]College of Public Health, Jinzhou Medical University, Jinzhou, China, [2]College of Bio informational Engineering, Jinzhou Medical University, Jinzhou, China, [3]College of Physics, Nankai University, Tianjin, China

A near-infrared fluorescent probe (LS-NO) for the real-time detection of nitric oxide (NO) in inflammatory bowel disease (IBD) was developed recently. The probe used oligoglycol morpholine-functionalized thiophene as strong electron donors and diaminobenzene (1,2,5-thiadiazole) as a weak electron acceptor and NO trapping group. It could detect exogenous and endogenous NO in the lysosomes of living cells with high sensitivity and specificity. To further understand the fluorescent mechanism and character of the probes LS-NO and LS-TZ (after the reaction of the probe LS-NO with NO), the electron transfer in the excitation and emitting process within the model molecules DAD-NO and DAD-TZ was analyzed in detail under the density functional theory. The calculation results indicated the transformation from diaminobenzene (1,2,5-thiadiazole) as a weak electron acceptor to triazolo-benzo-(1,2,5-thiadiazole) as a strong electron acceptor made LS-NO an effective "off–on" near-infrared NO fluorescent probe.

KEYWORDS

fluorescent probe, nitric oxide, inflammatory bowel disease, density functional theory, electron transfer

1 Introduction

Nitric oxide (NO) is a metastable free radical molecule which plays an important role in signal transduction and regulation in cardiovascular, immune, respiratory, gastrointestinal, and central nervous systems, and other physiological systems (Wang et al., 2002; Cosby et al., 2003). Recent studies have demonstrated that NO disorders are associated with a number of human diseases, including atherosclerosis, immune diseases, neurodegenerative diseases, cancer, and inflammatory bowel disease (Bogdan, 2001; Mel et al., 2011; Fmedsci, 2016). Moreover, increasing the NO concentration in the intestine is closely related to IBD (Kamalian et al., 2020). However, due to the lack of an effective method for the real-time detection of NO in the intestinal tract, the mechanism between NO and the pathogenesis of IBD remains unclear. Therefore, there is an urgent need to develop NO imaging probes with high sensitivity, high specificity, and high spatial and temporal resolution for the real-time detection of NO *in vivo* so as to further improve the diagnosis and treatment of IBD (Weissleder and Ntziachristos, 2003; Sasaki et al., 2005; Yu et al., 2012; Vegesna et al., 2013; Zhang et al., 2017). A near-infrared (NIR) fluorescent probe has more advantages in non-invasive imaging *in vivo*, which can further enhance the penetration of deep tissue and improve the signal-to-noise ratio (Antaris et al., 2016; Hong et al., 2017; Liu et al., 2021a; Wang et al., 2021; Xu et al., 2021). However, the current small-molecule fluorescent probes used for NO detection still have shortcomings such as short wavelength (<700 nm) and poor water solubility, especially in deep tissue and disease animal

10.3389/fchem.2022.990979

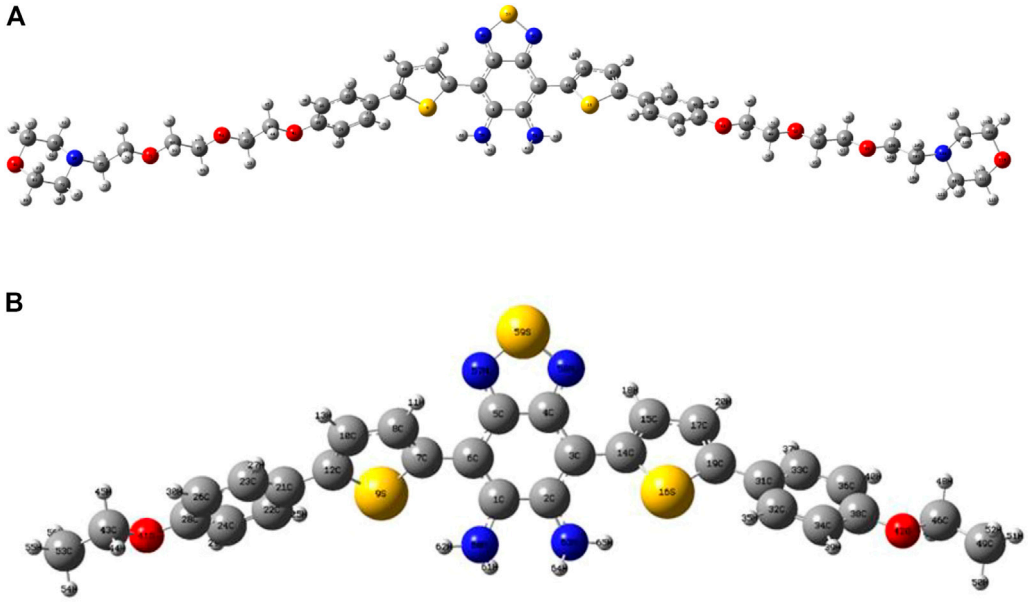

FIGURE 1
Optimized structures of **(A)** LS-NO and **(B)** DAD-NO.

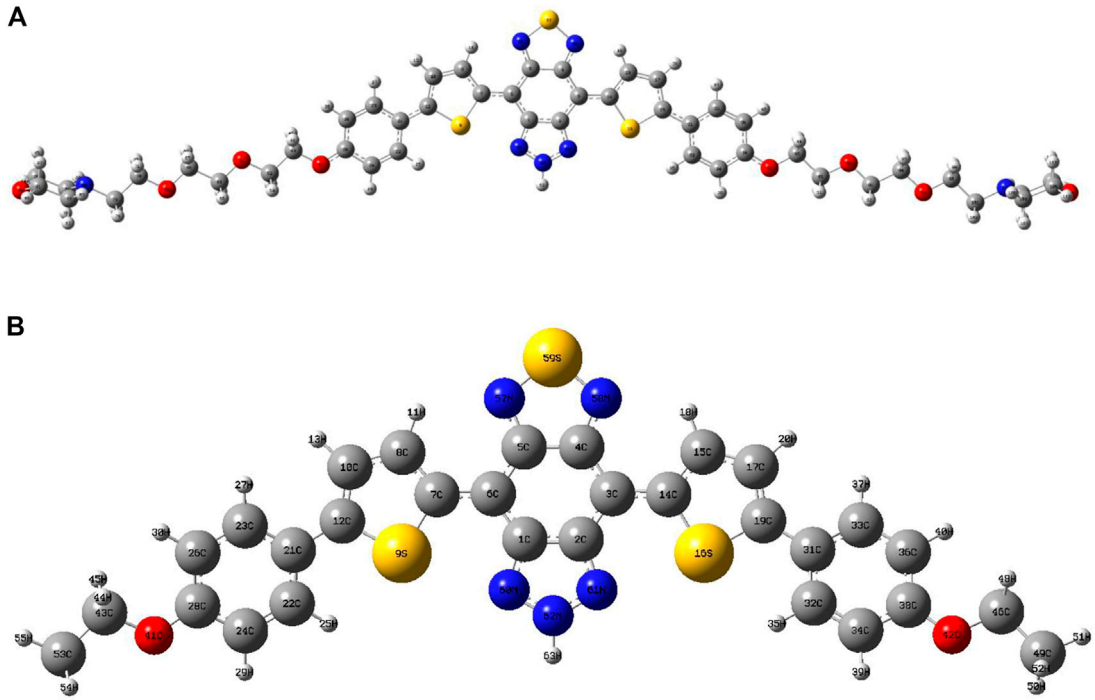

FIGURE 2
Optimized structures of **(A)** LS-TZ and **(B)** DAD-TZ.

models. It is still a great challenge to apply these probes to the real-time imaging detection of NO *in vivo* (Izumi et al., 2009; Li et al., 2016; Zhang et al., 2018).

A near-infrared fluorescent probe (LS-NO) for the real-time detection of NO in inflammatory bowel disease (IBD) was developed by Liu et al. (2021b). The probe used oligoglycol morpholine-functionalized thiophene as strong electron donors and diaminobenzene (1,2,5-thiadiazole) as a weak electron acceptor and NO trapping group. After the specific reaction of the probe with NO, the weak electron acceptor group diaminobenzene (1,2,5-thiadiazole)

10.3389/fchem.2022.990979

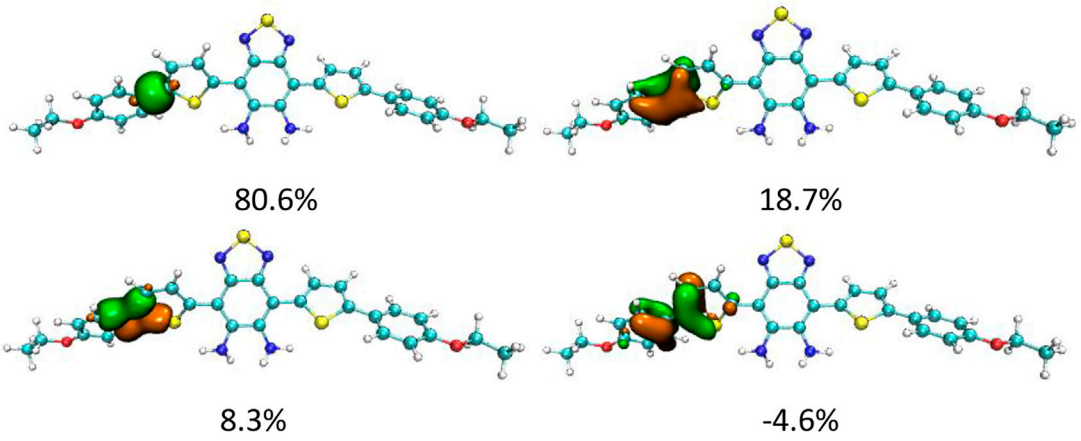

FIGURE 3
NAdO distribution of the *a*-related C–C bonds in DAD-NO.

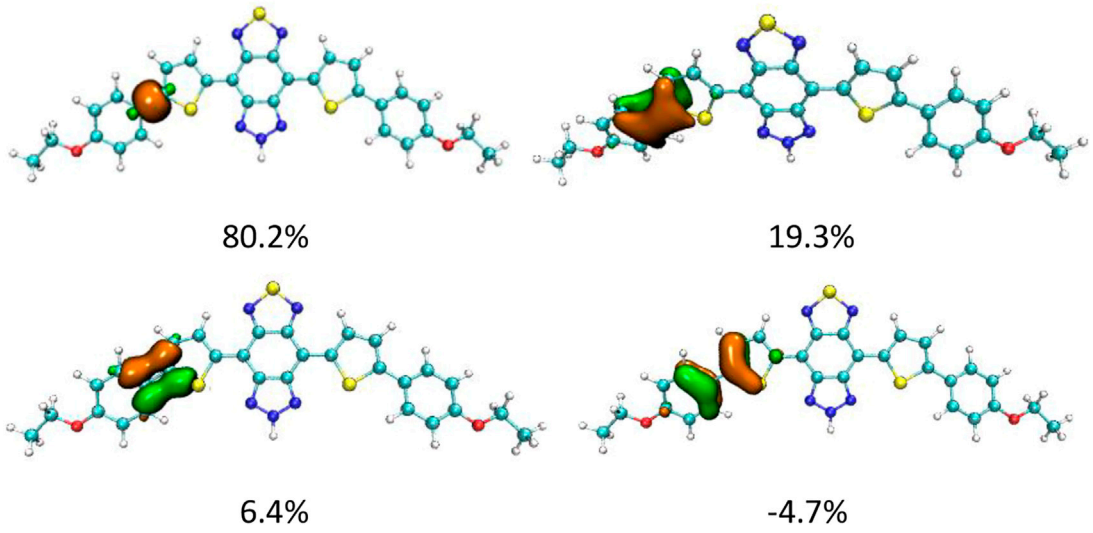

FIGURE 4
NAdO distribution of the *a*-related C–C bonds in DAD-TZ.

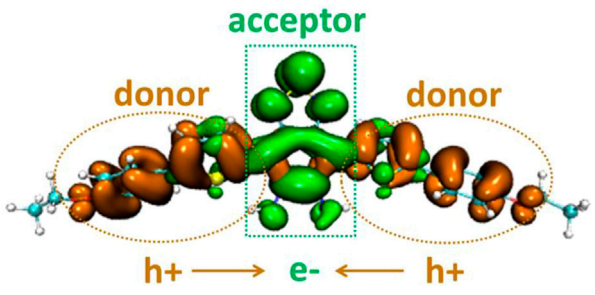

FIGURE 5
Electron distribution difference between S_0 and S_1 of DAD-NO (orange and green in the isosurface map represent the hole and electron distribution in the excitation process).

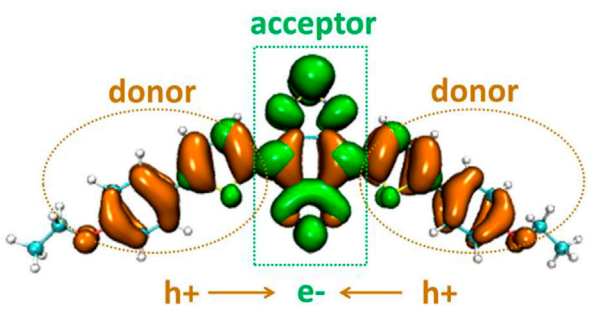

FIGURE 6
Electron distribution difference between S_0 and S_1 of DAD-TZ.

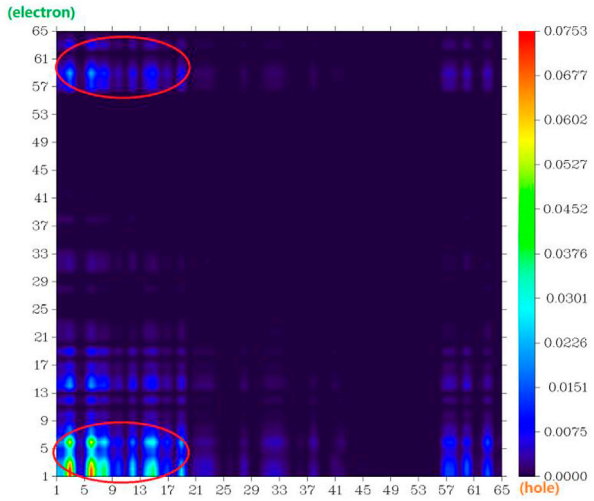

FIGURE 7
Atom–atom electron transfer heatmap of DAD-NO (atom numbers were referred to Figure 1).

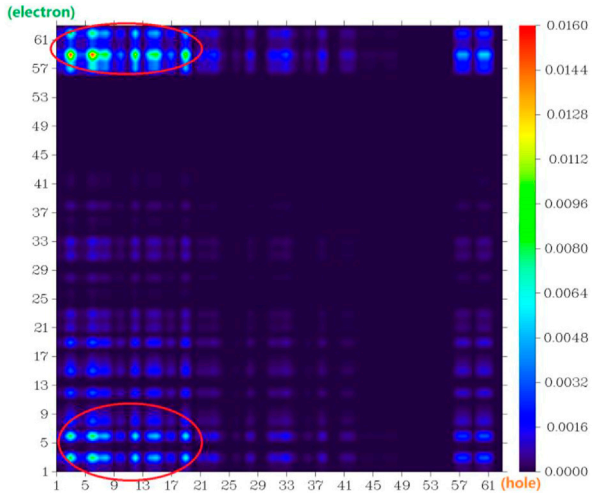

FIGURE 8
Atom–atom electron transfer heatmap of DAD-TZ (atom numbers were referred to Figure 2).

was transformed into the strong electron acceptor triazolo-benzo-(1,2,5-thiadiazole). By using the enhanced intramolecular charge transfer mechanism, the probe exhibited "off–on"-type near-infrared absorption and emission at 700 and 750/800 nm, respectively. In addition, LS-NO showed good water solubility and optical stability. It can detect exogenous and endogenous NO in the lysosomes of living cells with high sensitivity and specificity. This work suggested that LS-NO was promising as a diagnostic probe for the real-time detection of NO in IBD and may also facilitate inflammatory stool detection. To further understand the fluorescent mechanism and character of the probes LS-NO and LS-TZ (after the reaction of the probe LS-NO with NO), the electron transfer in the excitation and emitting process within the probe model molecules DAD-NO and DAD-TZ was analyzed in detail under the density functional theory. The calculation results indicated the transformation from diaminobenzene (1,2,5-thiadiazole) as the weak electron acceptor to triazolo-benzo-(1,2,5-thiadiazole) as the strong electron acceptor made LS-NO an effective "off–on" NIR NO fluorescent probe.

2 Methods

The ORCA 5.0.1 (Neese, 2018) software was used to perform optimization and vibrational frequency analysis on the S_0 structures of the model probes DAD-NO and DAD-TZ under PBE0/def2-TZVP with D3 dispersion correction (Adamo and Barone, 1999; Weigend and Ahlrichs, 2005; Grimme et al., 2011), and then single-point energy and TDDFT calculation under wB2GP-PLYP/def2-TZVP so as to obtain the free energy with high precision (Goerigk and Grimme, 2014; Casanova-Páez et al., 2019; Casanova-Paez and Goerigk, 2020; Peng et al., 2021; Liu et al., 2022). The functional PBE0-D3(BJ) and wB2GP-PLYP used for structure optimization and TDDFT calculation of such organic probe molecules were verified to be proper (Ali et al., 2020; Bremond et al., 2021; Santra and Martin, 2022). The optimized S_1 structures of DAD-NO and DAD-TZ were obtained under a combination of wB2GP-PLYP/def2-TZVP to analyze the emitting wavelength in the excitation and radiation process of the probe. All the figures were rendered by means of VMD 1.9.3 software (Humphrey et al., 1995) and the analyses were conducted using the Multiwfn 3.7 code (Lu and Chen, 2012).

3 Results and discussion

The optimized structures of probes LS-NO and LS-TZ with corresponding model probes DAD-NO and DAD-TZ are depicted in Figures 1, 2, respectively. In order to focus solely on the electron donor and acceptor parts in the probe, and to reduce computational time, the two terminal groups in the probes (LS-

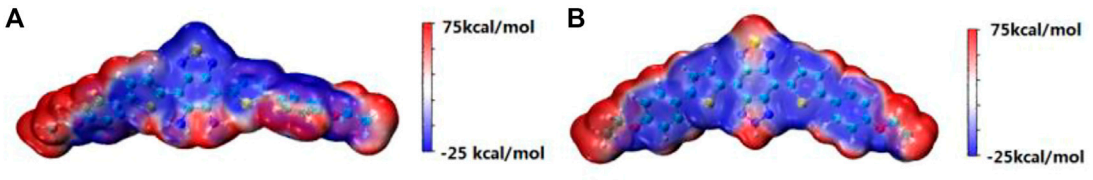

FIGURE 9
Electrostatic potential of **(A)** DAD-NO and **(B)** DAD-TZ.

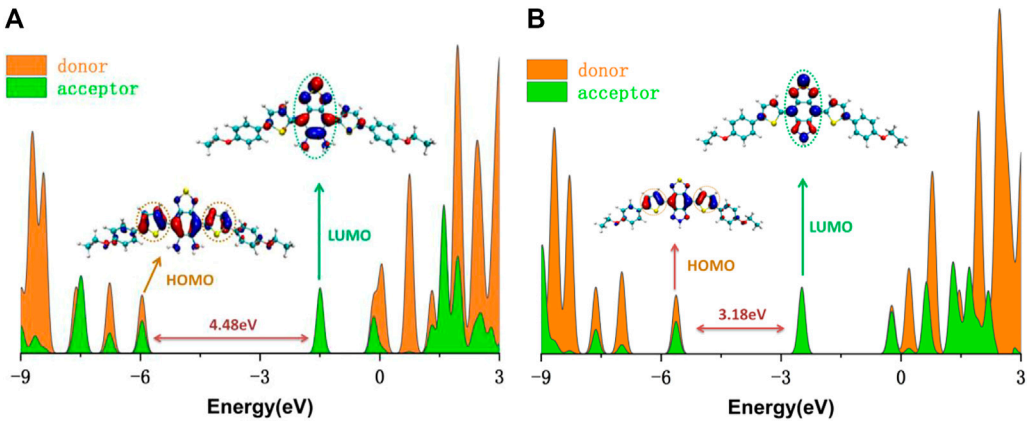

FIGURE 10
DOS of **(A)** DAD-NO and **(B)** DAD-TZ and the corresponding HOMO-LUMO energy gap calculated at the wB2GP-PLYP/def2-TZVP level in the gas.

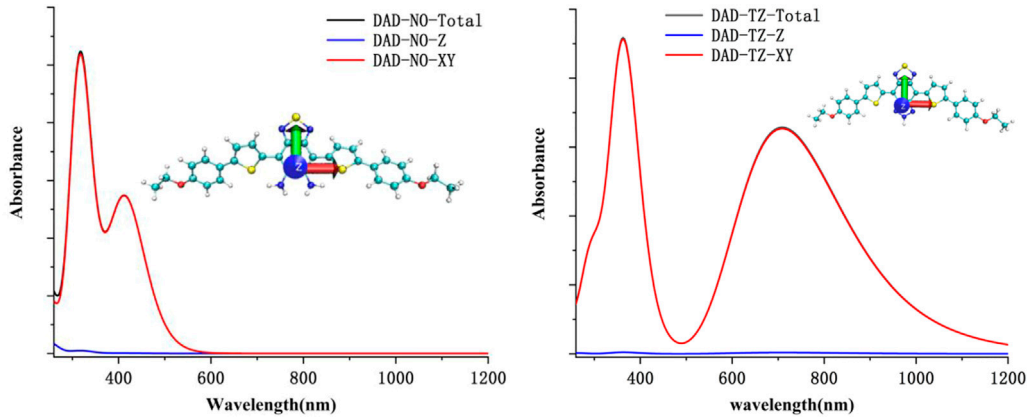

FIGURE 11
Calculated UV-Vis spectrum of DAD-NO and DAD-TZ in aqueous solution.

NO and LS-TZ) were cut to ethyl as shown in the model probes (DAD-NO and DAD-TZ).

The structures of the probes (as shown in Figures 1, 2) show that the DAD-NO had a more twisted structure than DAD-TZ, while the weak electron acceptor diaminobenzene (1,2,5-thiadiazole) was replaced by triazolo-benzo-(1,2,5-thiadiazole) as a strong electron acceptor.

Although DAD-NO had a more twisted structure than DAD-TZ, the α(β)-related C–C bonds shown in Figures 1, 2 were all typical C–C single bonds and had a similar natural adaptive orbital (NAdO) distribution (Zhang et al., 2020). The details of the NAdO distribution of the *a*-related C–C bonds in DAD-NO and DAD-TZ are shown in Figures 3, 4, respectively. The details of the NAdO distribution of *ß*-related C–C bonds in DAD-NO and DAD-TZ are given in Supplementary Figures S1, S2, respectively, for reference.

Figures 3, 4 show that the *a*-related C–C bond was a typical single C–C bond with main contribution from the localized sigma bond—about 80% in both DAD-NO and DAD-TZ. The second large contribution (about 19%) came from the pi bond which delocalized to the neighbor carbon atoms unlike the sigma bond. There were two other NAdOs which consist of *P* orbitals of carbon atoms with parallel and opposite phases, respectively, as shown in Figures 3, 4. The last two NAdOs displayed non-negligible contributions to the C–C bond with positive and negative values, respectively.

The electron distribution difference between the first excitation state and ground state of DAD-NO and DAD-TZ was obtained using Multiwfn 3.7 and depicted in Figures 5,6, respectively. The electron donor–acceptor–donor character in the probes could be clearly seen from the electron transfer process (from hole "h+" to electron "e−" as shown in Figures 5, 6). The electron acceptor parts in the probes mainly consist of N-contained and central hex-atomic rings, while the oxygen, five-membered and hex-atomic rings on the two sides contributed the donor parts in the probe.

The atom–atom electron transfer heatmap in the electron excited process of DAD-NO (Figure 7) and DAD-TZ (Figure 8) clearly

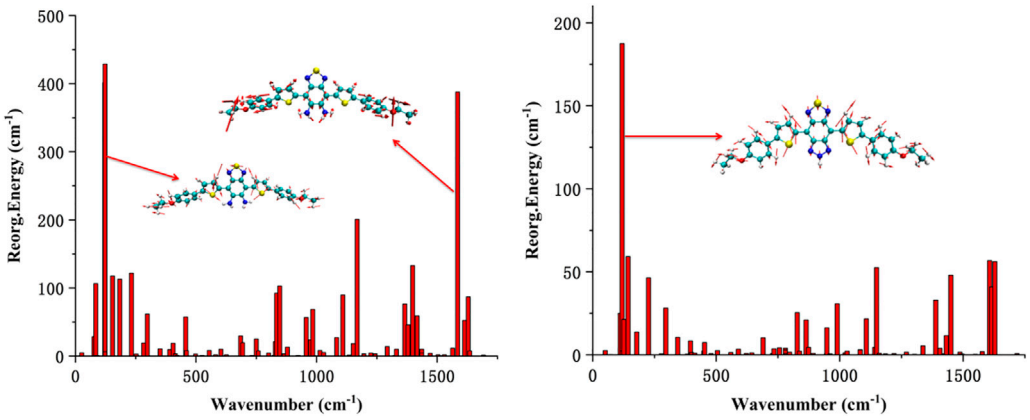

FIGURE 12
Calculated reorganization energy from each normal mode of DAD-NO and DAD-TZ.

indicated the obvious electron transfer from the donor parts to acceptor parts. The electrostatic potential of DAD-NO and DAD-TZ is shown in Figure 9. It could be also seen that the replacement of weak electron acceptor diaminobenzene (1,2,5-thiadiazole) by strong electron acceptor triazolo-benzo-(1,2,5-thiadiazole) made the electron acceptor part of DAD-TZ take a larger electrostatic potential value than DAD-NO.

To clarify the contribution of the donor and acceptor parts in DAD-NO and DAD-TZ to the density of electronic states, the DOS of DAD-NO and DAD-TZ and the corresponding HOMO-LUMO energy gap calculated at the wB2GP-PLYP/def2-TZVP level in the gas are depicted in Figure 10. It was obvious that the donor part's contribution to the HOMO exceeded that of the acceptor part, while the opposite situation happened within the LUMO. The replacement of diaminobenzene (1,2,5-thiadiazole) by triazolo-benzo-(1,2,5-thiadiazole) led to a smaller HOMO-LUMO energy gap which made the near-infrared fluorescence generation enhanced in DAD-TZ than in DAD-NO.

To understand the quantificational change in the energy and spectrum between DAD-NO and DAD-TZ, the UV-Vis spectrum of the probes in aqueous solution (a mixture of DMF/water with a volume ratio of 50/50) was analyzed using TDDFT calculation under the wB2GP-PLYP/def2-TZVP method. The calculated results are shown in Figure 11. As shown in Figure 11, there were absorption peaks located within the red and blue channels for DAD-TZ but only absorption peaks located within blue channels for DAD-NO which was consistent with the experimental results (Liu et al., 2021b). In addition, it could be clearly shown that the energy absorbance mainly located inside the probe molecular plane (XY plane) and the energy absorbance along the perpendicular direction to the molecular plane (*Z* axis) were almost negligible. This conclusion was consistent with the reorganization energy analysis between the ground and first excited states of DAD-NO and DAD-TZ in Figure 12. It could be clearly shown that the reorganization energy of DAD-NO was bigger than that of DAD-TZ, while the direction of the norm modes with most contribution were both parallel to the molecular plane in the two probes.

4 Conclusion

The geometric and electronic structures of the ground and excited states of an effective "off–on" NIR NO fluorescent model probe DAD-NO (DAD-TZ) were analyzed under the density functional theory in detail. The calculated results indicated that the transformation from diaminobenzene (1,2,5-thiadiazole) as a weak electron acceptor in DAD-NO to triazolo-benzo-(1,2,5-thiadiazole) as a strong electron acceptor in DAD-TZ made DAD-NO an effective "off–on" NIR NO fluorescent probe with high sensitivity and specificity. The electrostatic potential and density of electronic state analysis also suggested the changing of the electron acceptor part within DAD-NO, and DAD-TZ was the structural origin of the switch on/off of the NIR fluorescence in the probes. Energy absorbance mainly located inside the probe molecular plane (XY plane) and energy absorbance along the perpendicular direction to the molecular plane (*Z* axis) were almost negligible. All these theoretical results would provide an insight for designing new effective probes with similar functions.

Data availability statement

The original contributions presented in the study are included in the article/Supplementary Material; further inquiries can be directed to the corresponding author.

Author contributions

XL and SS collected the data; YL, QS, and JL contributed analytic tools and analyzed data; YP designed the research and prepared the manuscript.

Funding

This work was supported by the Undergraduate Innovation and Entrepreneurship Training Program of Jin Zhou Medical University

(2019055) and the Natural Science Foundation of Liaoning Province (2022-MS-389, JYTQN201923, and 20180550512).

Acknowledgments

Min Feng from Nankai University was appreciated for using GaussView 5.0 to draw Figures 1, 2.

Conflict of interest

The authors declare that the research was conducted in the absence of any commercial or financial relationships that could be construed as a potential conflict of interest.

Publisher's note

Supplementary material

The Supplementary Material for this article can be found online at: https://www.frontiersin.org/articles/10.3389/fchem.2022.990979/full#supplementary-material

References

Adamo, C., and Barone, V. (1999). Toward reliable density functional methods without adjustable parameters: The PBE0 model. *J. Chem. Phys.* 110, 6158–6170. doi:10.1063/1.478522

Ali, A., Rafiq, M. I., Zhang, Z., Cao, J., Geng, R., Zhou, B., et al. (2020). TD-DFT benchmark for UV-visible spectra of fused-ring electron acceptors using global and range-separated hybrids. *PCCP* 22, 7864–7874. doi:10.1039/d0cp00060d

Antaris, A. L., Chen, H., Cheng, K., Sun, Y., Hong, G., Qu, C., et al. (2016). A small-molecule dye for NIR-II imaging. *Nat. Mater.* 15, 235–242. doi:10.1038/nmat4476

Bogdan, C. (2001). Nitric oxide and the immune response. *Nat. Immunol.* 2, 907–916. doi:10.1038/ni1001-907

Bremond, E., Ottochian, A., Perez-Jimenez, A. J., Ciofini, I., Scalmani, G., Frisch, M. J., et al. (2021). Assessing challenging intra- and inter-molecular charge-transfer excitations energies with double-hybrid density functionals. *J. Comput. Chem.* 42, 970–981. doi:10.1002/jcc.26517

Casanova-Páez, M., Dardis, M. B., and Goerigk, L. (2019). ωB2PLYP and ωB2GPPLYP: The first two double-hybrid density functionals with long-range correction optimized for excitation energies. *J. Chem. Theory Comput.* 15, 4735–4744. doi:10.1021/acs.jctc.9b00013

Casanova-Paez, M., and Goerigk, L. (2020). Assessing the Tamm–Dancoff approximation, singlet–singlet, and singlet–triplet excitations with the latest long-range corrected double-hybrid density functionals. *J. Chem. Phys.* 153, 064106. doi:10.1063/5.0018354

Cosby, K., Partovi, K. S., Crawford, J. H., Patel, R. P., Reiter, C. D., Martyr, S., et al. (2003). Nitrite reduction to nitric oxide by deoxyhemoglobin vasodilates the human circulation. *Nat. Med.* 9, 1498–1505. doi:10.1038/nm954

Fmedsci, P. J. B. F. (2016). *J. Allergy Clin. Immunol.* 138, 16

Goerigk, L., and Grimme, S. (2014). Double-hybrid density functionals. *Wiley Interdiscip. Reviews-Computational Mol. Sci.* 4, 576–600. doi:10.1002/wcms.1193

Grimme, S., Ehrlich, S., and Goerigk, L. (2011). Effect of the damping function in dispersion corrected density functional theory. *J. Comput. Chem.* 32, 1456–1465. doi:10.1002/jcc.21759

Hong, G., Antaris, A. L., and Dai, H. (2017). Near-infrared fluorophores for biomedical imaging. *Nat. Biomed. Eng.* 1, 0010–0019. doi:10.1038/s41551-016-0010

Humphrey, W., Dalke, A., and Schulten, K. K. (1995). Vmd: Visual molecular dynamics. *J. Mol. Graph.* 14, 33–38. doi:10.1016/0263-7855(96)00018-5

Izumi, S., Urano, Y., Hanaoka, K., Terai, T., and Nagano, T. (2009). A simple and effective strategy to increase the sensitivity of fluorescence probes in living cells. *J. Am. Chem. Soc.* 131, 10189–10200. doi:10.1021/ja902511p

Kamalian, A., Asl, M. S., Dolatshahi, M., Afshari, K., Abdolghaffari, A. H., Roudsari, N. M., et al. (2020). Interventions of natural and synthetic agents in inflammatory bowel disease, modulation of nitric oxide pathways. *World J. Gastroenterol.* 26, 3365–3400. doi:10.3748/wjg.v26.i24.3365

Li, Z., Liu, Z., Zeng, L., Feng, W., and Mao and Zhiqiang (2016). *Chem. Sci.* 35, 2235

Liu, L.-Y., Zhao, Y., Zhang, N., Wang, K.-N., Tian, M., Pan, Q., et al. (2021). Ratiometric fluorescence imaging for the distribution of nucleic acid content in living cells and human tissue sections. *Anal. Chem.* 93, 1612–1619. doi:10.1021/acs.analchem.0c04064

Liu, S., Zhu, Y., Wu, P., and Xiong, H. (2021). Highly sensitive D–A–D-type near-infrared fluorescent probe for nitric oxide real-time imaging in inflammatory bowel disease. *Anal. Chem.* 93, 4975–4983. doi:10.1021/acs.analchem.1c00281

Liu, Y.-l., Huang, H., and Peng, Y.-j. (2022). Fluorescent probe for simultaneous detection of human serum albumin and sulfite: A theoretical analysis. *J. Mol. Struct.* 1255, 132441. doi:10.1016/j.molstruc.2022.132441

Lu, T., and Chen, F. (2012). Multiwfn: A multifunctional wavefunction analyzer. *J. Comput. Chem.* 33, 580–592. doi:10.1002/jcc.22885

Mel, A. D., Murad, F., and Seifalian, A. M. (2011). *Chem. Rev.* 111, 5742–5767. doi:10.1021/cr200008n

Neese, F. (2018). *Wiley Interdiplinary Rev. Comput. Mol. ence* 8, e1327.

Peng, Y. J., Huang, H., and Wang, C. J. (2021). DFT investigation on electronic structure, chemical bonds and optical properties of Cu6(SR)6 nanocluster. *Chem. Phys. Lett.* 780, 138898. doi:10.1016/j.cplett.2021.138898

Santra, G., and Martin, J. M. L. (2022). *J. Phys. Chem. Lett.* 13, 3499–3506. doi:10.1021/acs.jpclett.2c00718

Sasaki, E., Kojima, H., Nishimatsu, H., Urano, Y., Kikuchi, K., Hirata, Y., et al. (2005). Highly sensitive near-infrared fluorescent probes for nitric oxide and their application to isolated organs. *J. Am. Chem. Soc.* 127, 3684–3685. doi:10.1021/ja042967z

Vegesna, G. K., Sripathi, S. R., Zhang, J., Zhu, S., He, W., Luo, F.-T., et al. (2013). Highly water-soluble BODIPY-based fluorescent probe for sensitive and selective detection of nitric oxide in living cells. *ACS Appl. Mater. Interfaces* 5, 4107–4112. doi:10.1021/am303247s

Wang, K.-N., Liu, L.-Y., Mao, D., Xu, S., Tan, C.-P., Cao, Q., et al. (2021). A polarity-sensitive ratiometric fluorescence probe for monitoring changes in lipid droplets and nucleus during ferroptosis. *Angew. Chemie-International Ed.* 60, 15095–15100. doi:10.1002/anie.202104163

Wang, P. G., Xian, M., Tang, X., Wu, X., Wen, Z., Cai, T., et al. (2002). Nitric oxide Donors: chemical activities and biological applications. *Chem. Rev.* 102, 1091–1134. doi:10.1021/cr000040l

Weigend, F., and Ahlrichs, R. (2005). Balanced basis sets of split valence, triple zeta valence and quadruple zeta valence quality for H to Rn: Design and assessment of accuracy. *PCCP* 7, 3297–3305. doi:10.1039/b508541a

Weissleder, R., and Ntziachristos, V. (2003). Shedding light onto live molecular targets. *Nat. Med.* 9, 123–128. doi:10.1038/nm0103-123

Xu, W., Wang, D., and Tang, B. Z. (2021). NIR-II AIEgens: A win–win integration towards bioapplications. *Angew. Chem. Int. Ed.* 60, 7476–7487. doi:10.1002/anie.202005899

Yu, H., Xiao, Y., and Jin, L. (2012). A lysosome-targetable and two-photon fluorescent probe for monitoring endogenous and exogenous nitric oxide in living cells. *J. Am. Chem. Soc.* 134, 17486–17489. doi:10.1021/ja308967u

Zhang, C., Hu, S. X., Liu, H. T., Yang, Y., and Zhang, P. (2020). Correction to "bonding properties and oxidation states of plutonium in Pu_2O_n (n = 1–8) molecules studied by using screened hybrid density functional theory". *J. Phys. Chem. A* 124, 2513. doi:10.1021/acs.jpca.0c02144

Zhang, P., Tian, Y., Liu, H., Ren, J., Wang, H., Zeng, R., et al. (2018). *In vivo* imaging of hepatocellular nitric oxide using a hepatocyte-targeting fluorescent sensor. *Chem. Commun.* 54, 7231–7234. doi:10.1039/c8cc03240h

Zhang, R. R., Schroeder, A. B., Grudzinski, J. J., Rosenthal, E. L., Warram, J. M., Pinchuk, A. N., et al. (2017). Beyond the margins: Real-time detection of cancer using targeted fluorophores. *Nat. Rev. Clin. Oncol.* 14, 347–364. doi:10.1038/nrclinonc.2016.212